

RESEARCH ARTICLE | APRIL 20 2018

An original approach to elastic constants determination using a self-developed EMAT system FREE

Frédéric Jenot ; Frédéric Rivart; Liévin Camus



AIP Conf. Proc. 1949, 230018 (2018)

<https://doi.org/10.1063/1.5031665>



CrossMark

Articles You May Be Interested In

Multiple focused EMAT designs for improved surface breaking defect characterization

AIP Conference Proceedings (February 2017)

Enhanced surface defect detection using focused electromagnetic acoustic transducers (EMATs)

Proc. Mtgs. Acoust. (December 2017)

Comparison of a piezoceramic transducer and an EMAT for the omnidirectional transduction of SH₀

AIP Conference Proceedings (April 2018)

500 kHz or 8.5 GHz?
And all the ranges in between.

Lock-in Amplifiers for your periodic signal measurements



Find out more



An Original Approach to Elastic Constants Determination Using a Self-developed EMAT System

Frédéric Jenot^{1, a)}, Frédéric Rivart¹, Liévin Camus¹

¹*Univ. Valenciennes, CNRS, Univ. Lille, ISEN, Centrale Lille, UMR 8520 - IEMN Institut d'Electronique de Microélectronique et de Nanotechnologie, DOAE - Département d'Opto-Acousto-Electronique, F-59313 Valenciennes, France*

^{a)}Corresponding author: frederic.jenot@univ-valenciennes.fr

Abstract. Electromagnetic Acoustic Transducers (EMATs) allow non-contact ultrasonic measurements in order to characterize structures for a wide range of applications. Considering non-ferromagnetic metal materials, excitation of elastic waves is due to Lorentz forces that result from an applied magnetic field and induced eddy currents in a near surface region of the sample. EMAT's design is based on a magnet structure associated with a coil leading to multiple configurations, which are able to excite bulk and guided acoustic waves. In this work, we first present a self-developed EMAT system composed of multiple emission and reception channels. In a second part, we propose an original method in order to determine the elastic constants of an isotropic material. To achieve this goal, Rayleigh and shear waves are used and the advantages of this method are clearly highlighted. The results obtained are then compared with conventional measurements achieved with piezoelectric transducers.

INTRODUCTION

Materials characterization using non-contact ultrasonic methods is of great interest for many sectors of activity. Within this context, Electromagnetic Acoustic Transducers (EMATs) have been extensively used many scientific works related to non-destructive testing and evaluation. For example, EMATs allow the inspection of rail, gas pipeline and welded metal components keeping sensors a few millimeters above the structure [1-4]. EMATs are also able to directly excite in an electrical conductor, a large variety of ultrasonic waves including bulk and guided waves. EMATs interactions are based on two basic physical principles, which are magnetostriction and Lorentz force effects. Both have to be considered for ferromagnetic material but only the Lorentz force is important for other metallic materials. Several EMATs designs have been proposed and studied and these more often depend on the coil geometry used. In the literature, the longitudinal and shear directivity patterns of spiral, pancake and meander-line EMAT coils associated with an applied magnetic field in a given direction are also well described [5].

In this paper, we report experimental investigations in order to determine the elastic constants of a non-ferromagnetic isotropic material using a self-developed EMAT system. This device is first described and its main characteristics are highlighted. In a second part, the elastic parameters of the sample are obtained using an original approach based on simultaneous use of Rayleigh and shear waves. Finally, the improvement of the proposed method is discussed.

PRINCIPLES OF ELECTROMAGNETIC GENERATION AND DETECTION OF ULTRASONIC WAVES

We consider a coil with a circulating current I placed near the surface of a non-ferromagnetic conductive material. A magnetic field \mathbf{B} is applied to this coil using a magnet as shown in Fig. 1. In that case, the RF coil induced an eddy current density \mathbf{J} and the resulting Lorentz force \mathbf{F} is given by:

$$\vec{F} = \vec{J} \times \vec{B} \quad (1)$$

The direction of the magnetic field and the direction of the current in the coil allow Lorentz forces to excite different stresses in the sample [6]. Figure 1 shows two specific cases considering a magnetic field normal or parallel to the sample surface. The detection of acoustic waves is achieved by a similar coil-magnet system, thanks to the inverse process.

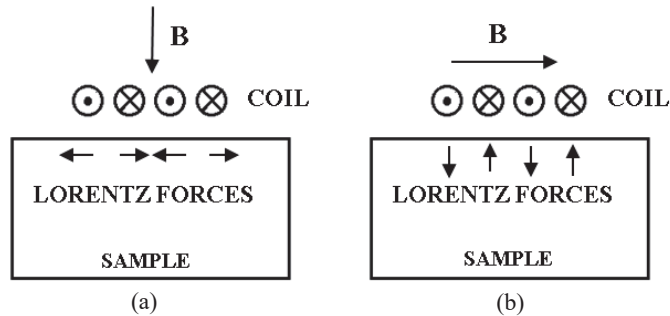


FIGURE 1. Basics of acoustic waves generation by EMATs. The applied magnetic field is normal to the sample surface (a) and parallel to the sample surface (b).

DESCRIPTION OF THE SELF-DEVELOPED EMAT SYSTEM

The self-developed EMAT system is mainly composed of three parts. The first part is a control unit including five electronic boards based on an FPGA processing architecture able to manage ten channels both in emission and in reception. This unit is connected to a computer through the USB port, and specific software allows piloting the whole system. This device is shown in Fig. 2.

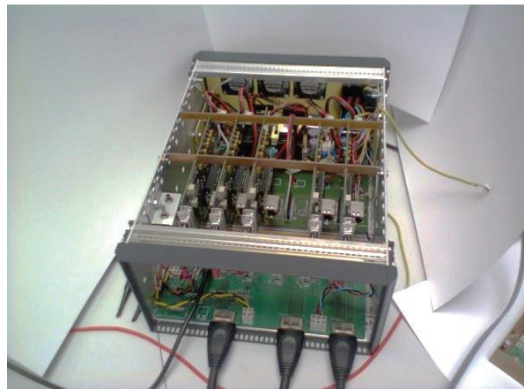


FIGURE 2. The control unit is composed of five electronic boards based on a FPGA processing architecture.

The second part is a remote currents generation unit composed of ten independent channels. Each emitter is able to deliver a high-current electrical pulse of 100 A and 300 ns duration (FWHM) directly into a large variety of sensors. This unit and the monopolar current pulse produced are presented in Fig. 3.

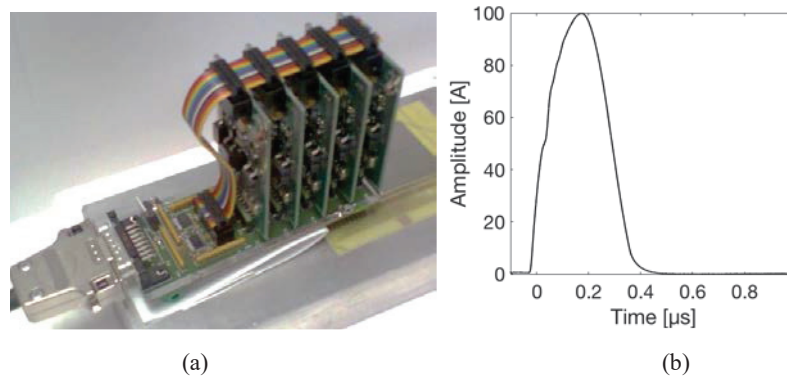


FIGURE 3. EMAT with its dedicated electronics (a). A 100 A monopolar current pulse and 300 ns duration (FWHM) is delivered to each sensor (b).

The last part consists of the electromagnetic transducers. The emitter and the receiver are each composed of the same type of segmented coil. This coil is based on a flat rectangular copper frame separated in ten elements as shown in Fig. 4. Considering the current direction in each element, which is driven by the unit previously described, the spatial periodicity of these elements is fixed to 1.8 mm.

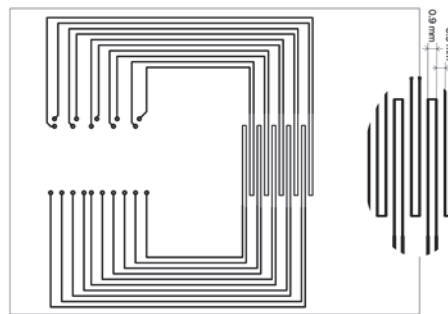


FIGURE 4. Schematic of the segmented coil used to form the EMATs. The right part is just an enlargement of the central zone for convenience only.

Two directions of the applied permanent magnetic field are then successively considered, and the configurations studied are those described in Fig. 1. To generate these fields, four identical parallelepiped magnets (40x20x5 mm) are placed side by side and put on the top of the segmented coil. The setup presented in Fig. 5 (a) allows obtaining a normal magnetic field to the sample surface. Only by rotating the magnets (Fig. 5 (b)), does the field become mainly parallel to this surface.

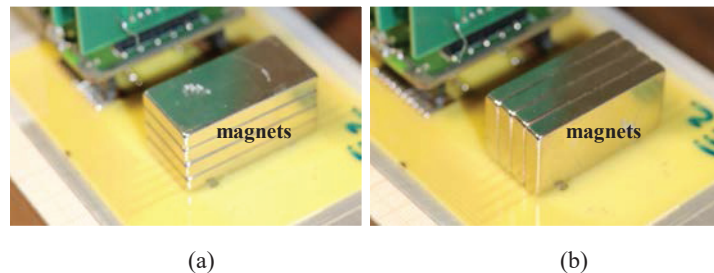


FIGURE 5. The magnetic field \mathbf{B} applied to the coil is normal to the sample surface (a). By rotating the magnets the field becomes mainly parallel to this sample surface (b).

The system also presents a time delay t_D between the emission of a current pulse and the beginning of signals acquisition. In order to determine this one, a wire is placed close to an excited element of the coil. Figure 6 shows

the electromagnetic signal induced in this wire and directly recorded using the developed interface. The time delay is measured at the maximum envelope of this signal. The value obtained is $t_D=22.54 \pm 0.15 \mu\text{s}$.

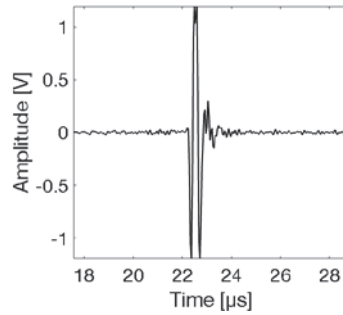


FIGURE 6. Electromagnetic signal induced in a wire placed close to an excited element of the coil.

EXPERIMENT

EMATs are positioned at the surface of an aluminum sample of 3.9 cm thickness and 2700 kg/m^3 density. As a first step, the applied magnetic field \mathbf{B} is mainly parallel to the sample surface and successive elements of the emitting coil are excited; the first one is denoted by E_0 . Concerning the receiving coil, only one element denoted by R is considered. The distance D between E_0 and R defined the shortest propagation path; its value is approximately 12 cm. Figure 7 shows the signals obtained considering three successively excited elements. The observed waveforms correspond to the Rayleigh wave.

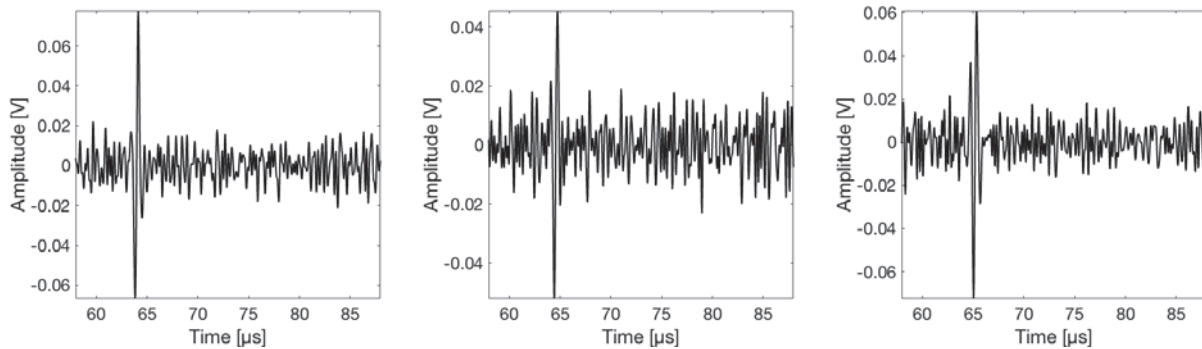


FIGURE 7. Rayleigh waveforms recorded for three successively excited elements.

In the second phase, the magnets are rotated in order to obtain a magnetic field \mathbf{B} normal to the sample surface. As before, the same three successive elements are used for the excitation of acoustic waves. The signals obtained are presented in Fig. 8. The first and second waveforms correspond respectively to the Rayleigh and shear waves. This last point will be discussed in the next part.

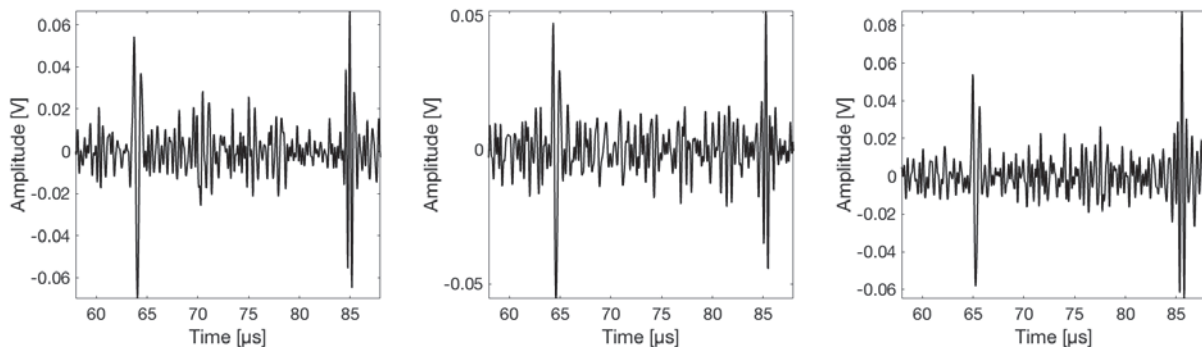


FIGURE 8. Rayleigh and shear waves detected for three successively excited elements.

RESULTS AND DISCUSSIONS

The first setup previously described is used to determine the Rayleigh wave velocity. Indeed, shear wave is not detected and in some particular cases (such as thinner samples investigation), that may avoid overlapping echoes due to the close velocities of shear and surface waves. Successive elements of the emitting coil are excited and the Rayleigh wave times of flight are measured using the zero-crossing method. Figure 9 shows the variation Δd of the propagation path versus the variation Δt of the Rayleigh wave time of flight. A linear fit of these variations is computed and the slope of the least-squares line corresponds to the Rayleigh wave velocity $V_R=2954.6$ m/s.

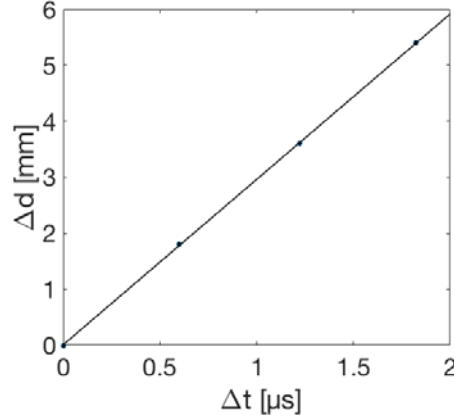


FIGURE 9. Variations of the propagation distance versus that of the Rayleigh wave time of flight. The surface wave velocity deduced is 2954.6 m/s.

When E_0 is the emitter, the time associated with the maximum amplitude of the Rayleigh waveform is $t_{MR}=64.12$ μ s. Considering the time delay t_D , the source-receiver distance D can be calculated taking into account the Rayleigh wave time of flight $t_{R}=t_{MR}-t_D$. This leads to $D=V_{R,tR}=12.28 \pm 0.05$ cm and this value is in good agreement with the expected distance.

The second setup is then investigated in order to obtain the shear wave velocity. The bulk wave propagation path is given in Fig. 10; P_S denotes its length.

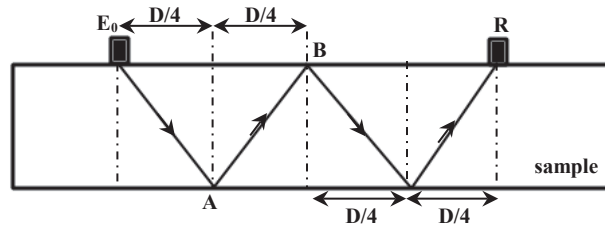


FIGURE 10. Shear wave propagation path.

This path has been checked by a finite element modeling (FEM) where E_0 is defined as a basic tangential forces dipole located at the sample surface. For this simulation, an aluminum sample of 4 cm thickness and 2700 kg/m³ density is considered. The Lamé elastic constants λ and μ of the material are, respectively, 58.1 GPa and 26.1 GPa. The propagation distance between E_0 and R is 12 cm and the normal displacement due to a pulse excitation is calculated at points A and B . The results are presented in Fig. 11. Rayleigh (R) and shear wave (S) are clearly observed, and their times of flight confirm the expected propagation path.

The distance D previously determined using the Rayleigh wave allows calculating P_S . The value obtained is $P_S=19.85$ cm \pm 0.03 cm. This leads to calculate the shear wave velocity V_S using the time $t_{MS}=84.96$ μ s associated with the maximum of the shear waveform when E_0 is the source. This velocity is given by $V_S=P_S/(t_{MS}-t_D)=3181 \pm 4$ m/s.

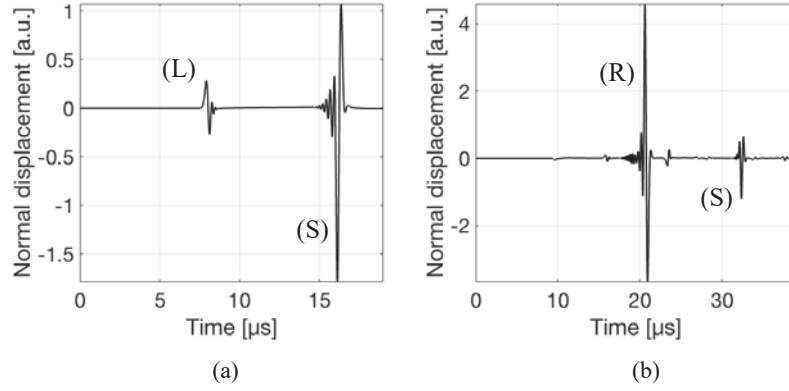


FIGURE 11. Longitudinal (L), shear (S) and Rayleigh (R) waveforms obtained by FEM considering an aluminum sample. The normal displacement is calculated at points A (a) and B (b).

Rayleigh and shear wave velocities permit to deduce the Poisson's ratio ν of the material. An approximated expression given by Royer is the following [7]:

$$\frac{\nu}{1-\nu} = \frac{0.58V_R^2 - 0.44V_S^2}{V_S^2 - V_R^2} \quad (2)$$

The solution of the previous equation leads to $\nu = 0.30 \pm 0.01$. The Poisson's ratio is also defined as:

$$\nu = \frac{V_L^2 - 2V_S^2}{2(V_L^2 - V_S^2)} \quad (3)$$

where V_L is the longitudinal bulk wave velocity. This leads to $V_L = 6008 \pm 66$ m/s.

Measurements have also been achieved using piezoelectric transducers operating in a pulse-echo mode. The longitudinal and shear wave velocities directly obtained are respectively 6309 m/s and 3082 m/s. The material density ρ allows the determination of the material elastic constants C_{11} , C_{12} and C_{44} according to the relations $V_L = (C_{11}/\rho)^{0.5}$ and $V_S = ((C_{11} - C_{12})/2\rho)^{0.5} = (C_{44}/\rho)^{0.5}$. Table 1 summarizes the results.

TABLE 1. Elastic constants determined using electromagnetic-acoustic method and conventional pulse-echo technique

Elastic Constants (GPa)	Electromagnetic-Acoustic Method	Pulse-Echo Technique
C_{11}	97.4 ± 2.3	107.5
C_{12}	42.8 ± 2.3	56.2
C_{44}	27.32 ± 0.06	25.6

These initial findings are encouraging and validate the proposed electromagnetic-acoustic method. The accuracy on the sample thickness measurement could be greatly improved in order to reduce the errors on velocities. It would also be possible to use different elements of the emitting coil with a well-chosen spacing in order to calculate the shear wave velocity without taking into account the system time delay.

CONCLUSION

In this study, a self-developed EMAT system has been presented. It allows the use of numerous transducers composed of varying coils and magnetic fields. An original approach based on simultaneous excitation and detection of Rayleigh and shear waves has demonstrated the potentiality of the proposed method in order to determine the elastic constants of homogeneous and isotropic materials. This study clearly shows the advantage of a segmented coil excited in pulse mode. It was also possible to easily select one of the previous acoustic waves by changing the applied magnetic field direction. In some particular cases, this is interesting to avoid overlapping signals. Further work is, however, needed to increase the measurements accuracy, and a new coil will be designed to that end. Studies about directional characteristics of specific transducers are also under way.

ACKNOWLEDGMENTS

The present research work has been partially supported by the National Research Agency (ANR). The authors gratefully acknowledge the support of this institution.

REFERENCES

1. S. Dixon, C. Edwards, S.B. Palmer, "A laser-EMAT system for ultrasonics weld inspection," *Ultrasonics* **37**, 273-281, (1999).
2. P.A. Petcher, M.D.G. Potter, S. Dixon, "A new electromagnetic acoustic transducer (EMAT) design for operation on rail," *NDT E Int.* **65**, 1-7 (2014).
3. M. Hirao, H. Ogi, "An SH-wave EMAT technique for gas pipeline inspection," *NDT E Int.* **32**, 127-132, (1999).
4. W. Luo, J.L. Rose, "Guided wave thickness measurement with EMATs," *Insight*, **45**, 1-5, (2003).
5. J.K. Hu, Q.L. Zhang and D.A. Hutchins, "Directional characteristics of electromagnetic acoustic transducers," *Ultrasonics*, **26**, 5-13, (1988).
6. H.M. Frost, "Electromagnetic-ultrasound transducers: principle, practice and applications," in *Physical Acoustics*, (eds.) W.P. Masson and R.N. Thurston, Academic Press, New York, **14**, 179-275, (1979).
7. D. Royer, D. Clorennec, "An improved approximation for the Rayleigh wave equation," *Ultrasonics*, **46**, 23-24, (2007).